

# Preliminary Design of a Horizontal Axis Tidal Turbine for Low-Speed Tidal Flow

Job Immanuel Encarnacion<sup>1</sup>, Cameron Johnstone<sup>2</sup>

*Mechanical and Aerospace Engineering, University of Strathclyde  
Glasgow, United Kingdom*

<sup>1</sup>job.encarnacion@strath.ac.uk

<sup>2</sup>cameron.johnstone@strath.ac.uk

**Abstract**— The renewable energy in the Philippines has a very low share in the country's power generation. It is then determined that the total potential of tidal in-stream energy in the Philippines is more than 80GW, which is more than enough to supply the 75GW target ORE capacity by 2025. However, the tidal flow around the country averages only at about 0.40-0.80m/s. This inhibits the development of tidal turbine technology since TSTs are currently very expensive and the low velocity flow will translate to very low energy captured per turbine. Thus, a preliminary blade design that is optimized for low velocity flow is implemented using computer simulations. Low velocity flow allows for the usage of high-tip speed ratio blades since cavitation is not a big issue; the linear speed of the blade is low even if the blade is operating at a high tip speed ratio. The NACA 63-8xx series blades are able to have maximum Cp values at higher tip speed ratios (TSR > 5.5). The study investigates the blades as they are made more slender to enable maximum output at even higher tip speed ratios (TSR = 7). The most slender blade is found to have a lower power output relative to the base case although the decrease is only at 3%. Thrust loads are also lower, however, the smaller cross-sectional area results in higher stresses. Nonetheless, static load simulation shows that the stresses are well below the allowable yield stress of a typical GFRP blade. This means that the slender blade may be considered in a low speed tidal flow condition and minimisation of cost due to lower loads and lower torque requirements for generators.

**Keywords**— HATT, Low-speed Flow, Design Optimization, BEM, Static Load

## I. INTRODUCTION

As of 2016, power generation from coal-fired plants still dominate the Philippine energy mix at 47.7% of the total energy share. The renewable sector only accounts for 24.2% with 12.2% coming from geothermal energy [1]. It is envisioned that 75MW of ocean energy is added by 2025 [2]. Tidal in-stream energy is a viable option for the country with a total potential of 80GW [3].

However, the average tidal current velocity in the Philippines ranges from 0.40-0.80m/s with a peak of 1.6m/s at San Bernardino Strait [4]. This inhibits the adoption of tidal turbine technologies in the country since there is an apparent lack in a suitable turbine blade design for low velocity tidal flow.

Current studies in the Philippines usually involve the adoption of existing turbine technologies with a cut-in speed that matches the average range of tidal velocities [4]. This is

misleading as existing technologies are not specifically designed for low velocity flow.

Thus, a design for tidal turbines operating in low velocity flows is done to enable the capture of tidal energy in regions such as the Philippines.

## II. NUMERICAL ANALYSIS OF BLADE PERFORMANCE

### A. Applied Blade Element Momentum Method

BEM is used to analyse the torque and the thrust on the blades. A code written in Python, adapted from Nevalainen [5], is used to implement BEM methods on a steady state flow velocity flow of 0.4 m/s. Two blade profiles are analysed, the NREL S814 blade by Barltrop [6] and the NACA 63-8XX series blade by Bahaj [7]. These blade profiles are chosen due to the occurrence of their peak Cp at different TSRs – at relatively low (TSR  $\approx$  4) and relatively high (TSR  $\approx$  5)TSRs respectively. The comparison is done to determine how a low-tip speed ratio and high-tip speed ratio blade would fair in a low velocity environment; and which would be more suitable to use for low velocity tidal flows.

The BEM method is then incorporated into the blade design methodology to come up with an optimized blade profile for low velocity flow. Gracie-Orr [6] developed a blade design methodology for over-speed regulation which limits the operation of turbines at low TSRs. This methodology serves as a basis for developing the appropriate blade profile for low velocity flows and the TSR region is determined by the initial comparison of the high and low TSR blades. It is worth noting that cavitation becomes an issue on high TSRs when a turbine is used in high velocity flow [6]. This effect is reduced for turbines operating in low velocity flows since higher TSRs do not result in angular speeds as high as the ones achieved for higher TSRs at high flow velocity.

### B. Blade Modifications

The base chord distribution, twist distribution, and characteristic airfoil for each control section are defined by [7] and [8], which are shown in Figures 1 and 2. The values of each chord and twist are then scaled by the calculated coefficients for two conic sections ( $x^2 + cxy + y^2 = a^2$ ): an ellipse ( $c < 1$ ) and a hyperbola ( $c > 1$ ). The y-values at the minimum and maximum control location are fixed to match the values of each

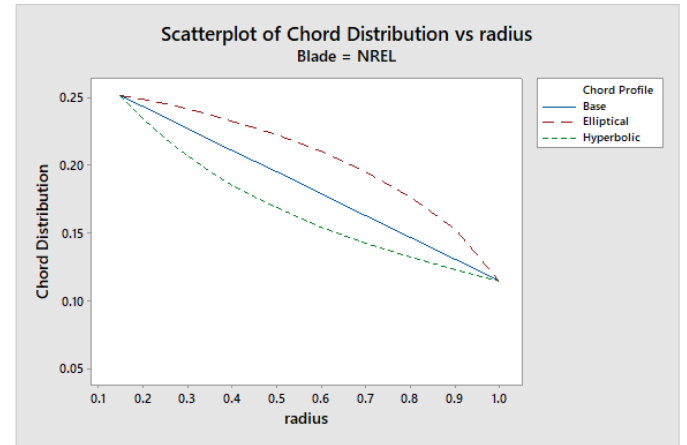
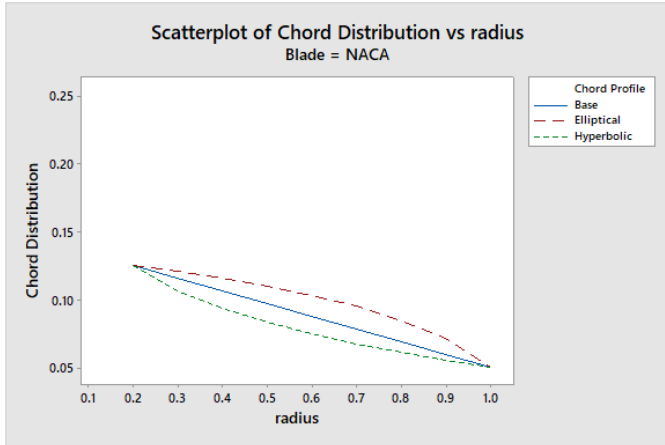
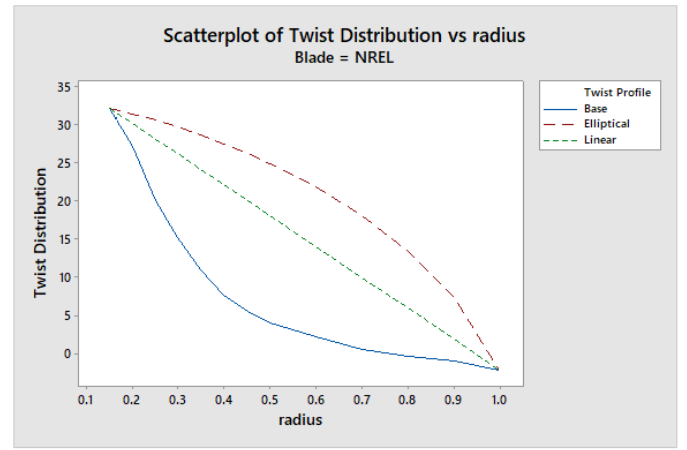
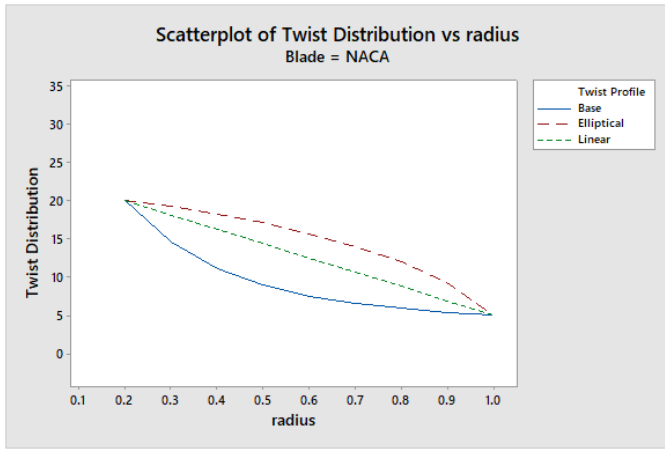


Figure 1. Twist and Chord Distributions of the NACA Blades

Figure 2. Twist and Chord Distributions of the NREL Blades

base case at  $r_{min}$  and  $r_{max}$ . The radius of the rotor is set to 4m to simulate an actual concept turbine operating in the ocean.

The base chord distribution differs in form/trend from the base twist distribution. A linear trend is seen for the base chord distribution while a trend similar to the elliptical profile is seen for the base twist distribution. Thus, the twist distribution is altered according to:

- base (elliptical),
- linear and,
- hyperbolic;

while the chord distribution is altered according to:

- elliptical,
- base (linear) and,
- hyperbolic

At most three candidate blade profiles are selected according to the following criteria:

- Maximum  $C_p$
- TSR where maximum  $C_p$  occurs; higher is better

The thrust coefficient is not included as a primary criterion since the thrust loads have a lower variation compared to the  $C_p$  ( $C_t \propto V^2$ ,  $C_p \propto V^3$ ).  $C_t$  is monitored and is only considered an indicator if there are too many candidate blade profiles. This serves as an initial investigation on the effects of altering the

distribution along the blade affects the hydrodynamic performance of the blade.

The three candidate NACA blades are then subjected to further alteration. These blades are made to be more slender to allow the maximum  $C_p$  value move towards higher TSRs [9]. From Figure 1, it is apparent that the NACA blades are already more slender than the NREL blades. The NREL blades are also made to be slightly more slender. The same percentage of the base chord length was removed, resulting in different absolute reduction.

### C. Candidate Selection

Figure 3 and 4 shows the performances of each blade as the respective alterations on twist and chord distributions are implemented. The BEM simulation do not result to a smooth curve. However, the general trend is followed and the performance of the blade is aptly captured.

The alteration results in three performance clusters for each blade. The clusters are dictated by the twist profile, and smaller variations within each cluster depends on the chord profile. This shows that the effect of altering the twist distribution is greater in compared to altering the chord distribution. However, the results for the NACA and the NREL blade differ as the base twist profile maximizes the  $C_p$  values for the NACA blade

while adopting a linear twist distribution is optimal for the NREL blade.

The maximum  $C_p$  of the NACA and NREL blades do not vary much in their optimized twist distribution forms. However, the location of the maximum  $C_p$  within the range of TSR varies and is shown in Figures 3 and 4. The hyperbolic chord distribution pushes the location of the maximum  $C_p$  to the higher TSRs; the effect is more pronounced for the NACA blade. This is expected since adopting a hyperbolic chord distribution results in a more slender blade. However, there is no decrease in simulated performance when adopting an elliptical chord distribution, opposite to the expected behaviour. The elliptical chord distribution may be seen as a simplification of the chord distribution and should result in a loss in efficiency [10]. However, the increased surface area may actually offset the loss in efficiency and result in only a small variation in maximum  $C_p$  relative to the base case.

The blade profiles selected for further analysis and comparison are then the base twist distribution NACA blades and the linear twist distribution NREL blades.

#### D. Optimized Blade Performance

The NACA and the NREL blades are reduced by 37.5% (average of 25-50%) of their original size. Tables 1 and 2 show the blade profile of the NACA and NREL blades used at this stage of the study. The range of TSR investigated for the NACA is extended,  $TSR = 2.75$  to 11, to accommodate for higher TSRs since it is expected that the blade will have maximum performance at even higher TSRs.

Table 1. Slender NACA blade profiles

r/R	twist	c/R		
		Ell	Base	Hyp
0.2	20	0.106	0.106	0.106
0.3	14.5	0.102	0.097	0.088
0.4	11.1	0.097	0.088	0.075
0.5	8.9	0.092	0.078	0.065
0.6	7.4	0.085	0.069	0.056
0.7	6.5	0.076	0.059	0.049
0.8	5.9	0.066	0.050	0.043
0.9	5.4	0.053	0.041	0.037
1	5	0.031	0.031	0.031

1) *NACA Blade*: Decreasing the overall chord length results in a decrease in the overall  $C_p$  of each of the blades. The maximum  $C_p$  are decreased by 0.6%, 3.2%, and 5.5% for the elliptical, base, and hyperbolic chord distribution blades of the more slender blade relative to the original NACA blades with the same chord distribution. Nonetheless, these  $C_p$  are still within practical range. Figure 5a shows the plot of the  $C_p$  versus TSR of the three slender NACA blades.

Table 2. Slightly Slender NREL Blade Profiles

r/R	twist	c/R		
		Ell	Base	Hyp
0.1494	32.1856	0.2092	0.2092	0.2092
0.1987	30.1896	0.2063	0.2012	0.1928
0.2506	28.0913	0.2028	0.1928	0.1776
0.2975	26.1977	0.1993	0.1852	0.1655
0.3494	24.0994	0.1950	0.1768	0.1536
0.3987	22.1035	0.1905	0.1688	0.1435
0.4506	20.0052	0.1854	0.1604	0.1341
0.5000	18.0092	0.1800	0.1524	0.1260
0.5987	14.0173	0.1677	0.1364	0.1119
0.7000	9.9230	0.1525	0.1200	0.0997
0.8000	5.8800	0.1340	0.1038	0.0892
0.9013	1.7857	0.1095	0.0874	0.0797
1.0000	-2.2062	0.0714	0.0714	0.0714

The location of the maximum  $C_p$  within the range of TSRs tested were also pushed further towards higher values. The location of the maximum  $C_p$  moved from a range of (4,5.5) to a range of (5.25,8.5). This should allow for increased angular speeds and decreased torque requirements for generators installed within the turbine.

The movement of the location of the maximum  $C_p$  as an effect of the alteration in the blade profile is also more pronounced in the more slender blade with the hyperbolic, or the most slender of the three, having its maximum  $C_p$  at  $TSR = 7.25$ , while the elliptical and the base chord distributions have their maximum  $C_p$ s at  $TSR = 6$  and  $TSR = 7$ , respectively. Comparing the slender blades' performance relative to each other, there is a decrease in power output of 3.5% with the hyperbolic chord distribution, with respect to the maximum power output of the base chord distribution. Conversely, there is an increase in power output of 3.3% with the elliptical chord distribution, with respect to the maximum power output of the base chord distribution.

Thrust loads are generally greater for the elliptical chord distribution blade, and decreases as the blade is made to be more slender. This is also probably due to the increased surface area that fluid interacts with. However, the general trend of  $C_t$  with respect to the TSR has changed from decreasing in the base case scenario (Figure 3) to a proportional increase. The average thrust loads increases by a factor of 11.5% for the elliptical chord distribution and decreases by a factor of 8.5% for the hyperbolic chord distribution, with respect to thrust

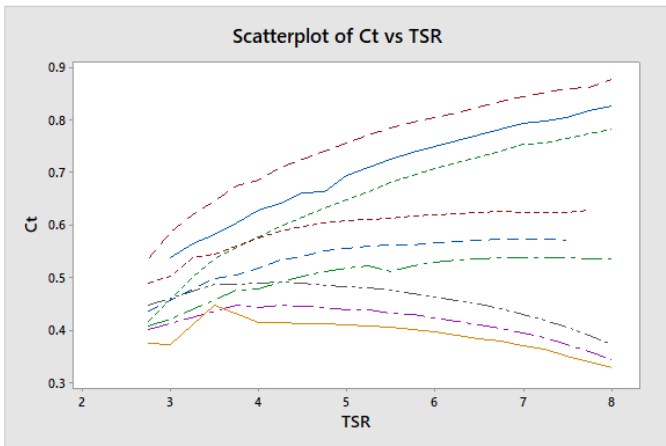
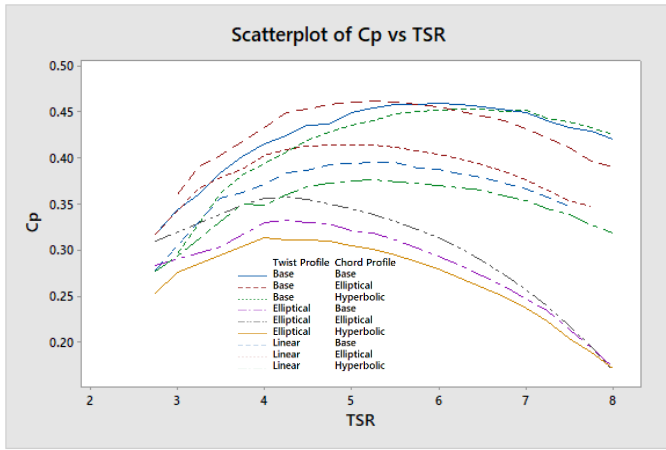


Figure 3. Cp and Ct vs TSR plots of the NACA blades

loads of the base chord distribution. Figure 5b shows the plot of the Ct versus TSR of the three blades.

2) *NREL Blade*: The slight slender NREL blades exhibit almost the same Cp trend with the slender NACA blades. However, there is an increase in maximum Cp when the NREL blades are made to be slightly slender. The maximum Cp of each blade has increased by 2.5%, 6.7%, and 3.1% for the elliptical, base, and hyperbolic chord distribution blades relative to the original NREL blades with a linear twist distribution and the same chord distribution.

Another difference is observed with the variation of Cp between the elliptical and base chord distribution blades. The base chord distribution blade has the highest maximum Cp, 2.2% more than the maximum Cp of the hyperbolic chord distribution blade, and 0.2% more than the elliptical chord distribution blade. However, the maximum Cp occurs within a spike in the simulated performance and it is possible that exactly the same trend may be observed in reality. Additionally, the movement of the location of the maximum Cp towards higher TSR was not present. Similar to the base case of the NACA (Figure 1 and 3), the movement may be insignificantly small due to blade having a large surface area, and thus, the effect may not be evidently perceived. Figure 6a then shows the plot of the Cp versus TSR of the three NREL blades.

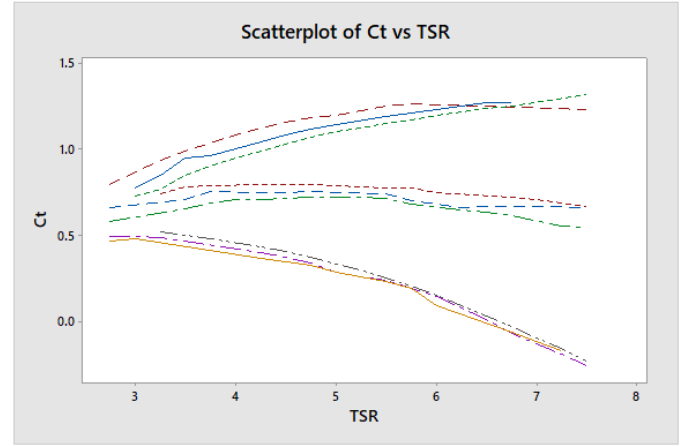
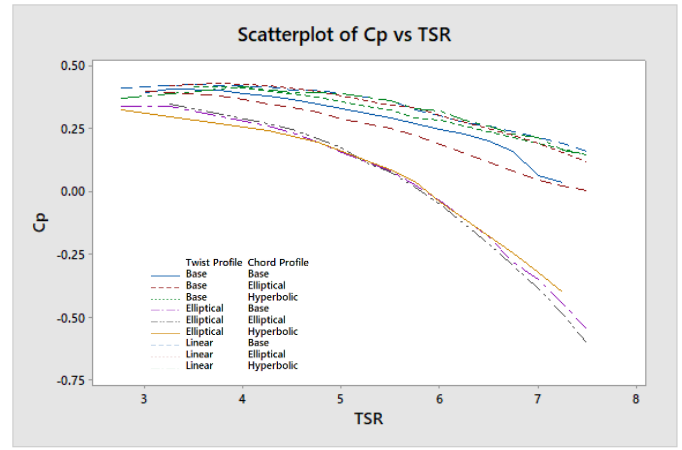


Figure 4. Cp and Ct vs TSR plots of the NREL blades

Thrust loads also follow the same general trend when changing from an elliptical chord distribution (slender) to a hyperbolic chord distribution (increased surface area). The hyperbolic chord distribution blade sees a decrease of 7.8% in the thrust loads while the elliptical chord distribution blade sees an increase of 9.1% increase in thrust loads. Figure 6b then shows the plot of the Ct versus TSR of the three NREL blades.

The performance of the slender NACA blade is desirable for low velocity flow. Comparing the performance of each blade with the same chord distribution, the slightly slender NREL blade tops the performance of the slender NACA blade by 2.0% and 0.6% for the base and hyperbolic chord distribution blades respectively. However, the elliptical chord distribution slender NACA blade has a greater maximum Cp of 4.2% more than the slightly slender NREL blade with the same chord distribution. These differences are not large but a structural analysis must be undertaken to determine the structural feasibility of the NACA blades on low speed tidal flow considering that the cross section of the blades have been greatly reduced.

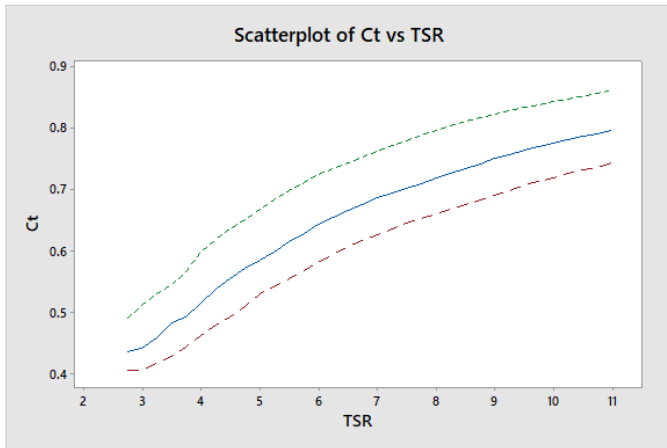
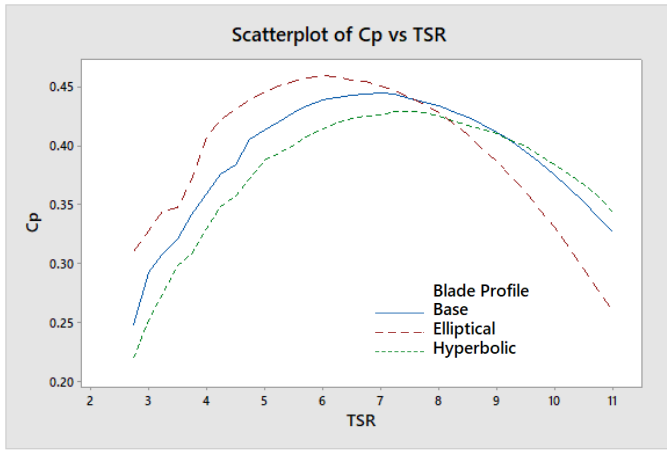


Figure 5. Cp and Ct vs TSR plots of the Slender NACA blades

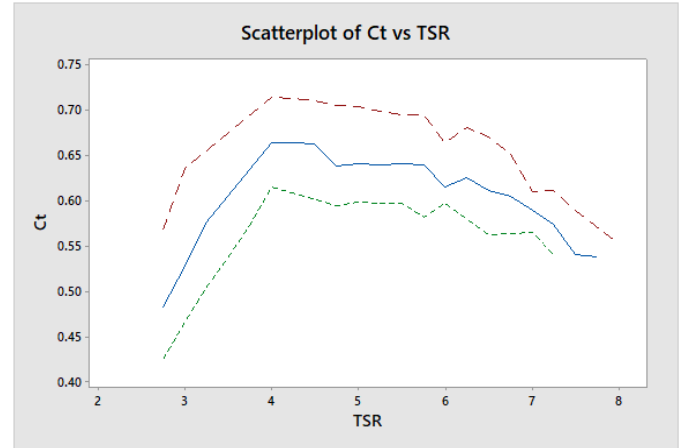
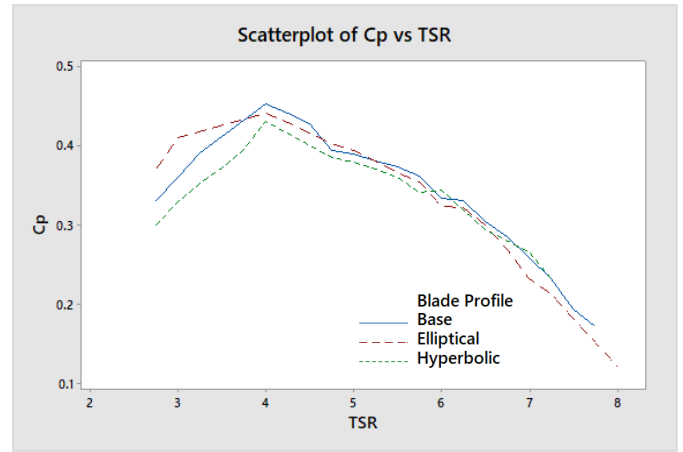


Figure 6. Cp and Ct vs TSR plots of the Slightly Slender NACA blades

### III. STATIC LOAD SIMULATION

#### A. Static Simulation Setup

Making the blade more slender have resulted in a desirable  $C_p$  at higher TSR. The slender blade has less cross sectional area and must be tested for structural feasibility. Hence, a static load simulation is performed to determine the stress and strain embodied in the blade as a result of hydrodynamic forces. A static load is appropriate at this point since heavy CFD simulations may be too computationally expensive at this early point. The CFD simulations may then be carried out after the blades have been filtered out - failure in the static regime, with an applied factor safety of at least five, implies that the blade is not suitable for operation.

The resulting axial and tangential force distribution on the blade are inputted into a CAD simulation where the blade is fixed at the onset of the aerodynamic section as shown in Figure 10. The material is set to be a typical glass fibre with a strength of 1186MPa. The loads are maximized using a tidal flow of 1.5m/s at the TSR where the maximum loads are felt. This should be the extreme case and non-failure in this regime should result in non-failure for lower speed regimes. Figure 7 gives a sample visualization of how loads vary for the NREL and NACA blades with respect to TSR.

#### B. Blade Stress

The stress on all the NACA and NREL blades are well below the yield stress and thus, it has passed the initial structural simulated testing. The loads observed in the hyperbolic chord distribution slender NACA blade is 153% more than the base chord distribution case. The elliptical chord distribution blade, despite it having a larger cross section, also sees 43% more stress compared to the base chord distribution, which may be attributed to the larger loads on the blade.

The NACA blades are loaded 3.49x more than the NREL blades. For both the NACA and NREL blades, the location of the stress concentration moves from near the root towards the tip of the blade as the blade becomes more slender. The hyperbolic chord distribution blades have the maximum stress located at the centre in this case. Nonetheless, the usual material may still be used as per the static simulation, and no alteration on blade material is needed. The slender blades should result in reduction in material needed for the blades in low velocity flow. Figures 8 through 13 show the stress distribution on the blades.

#### IV. CONCLUSIONS AND FUTURE WORK

A preliminary design for a tidal turbine for low-speed tidal flow has been conducted. The numerical simulations for the performance show reasonable  $C_p$  and  $C_t$  values of a more slender blade that is able to achieve optimum performance at higher TSRs. There is a decrease of 0.6-5.5% when the NACA blade is made to be more slender but the maximum  $C_p$  is pushed towards higher ranges of TSR (TSR = 6, 7, 7.25), which is desirable to decrease the torque requirements, and thus the physical size of the generator and the turbine housing. The stresses on the blades are 3.5x higher compared to the NREL blade even if the NREL blade was also made to be slightly more slender. However, the static simulation showed the blades are able to withstand yielding and hence, may be further tested for dynamic testing on the loads.

The technical feasibility of the blades in terms of power and structural performance has been shown. Further analysis is needed to assess the economic feasibility of the blades, with consideration to the generator sizing, housing, and other structural components. The stress on the blades are higher but the loads observed are generally lower than the base (slender) case blades when operated at low speed tidal flow.

#### ACKNOWLEDGMENT

The authors would like to thank the University of Strathclyde for the use of facilities and the Philippine Department of Science and Technology (DOST) – Engineering Research and

Development for Technology (ERDT) for funding provided in the form of study grants.

#### REFERENCES

- [1] Posadas, J.C. (2017). Philippine Energy Plan 2017-2040. Presentation to ACD Conference toward Energy Security, Sustainability and Resiliency
- [2] Delos Santos, A.S.A (2011). Renewable Energy in the Philippines. Presentation. International renewable Energy Agency.
- [3] Abundo, M.L.S (2016). Marine Renewable Energy for Island Micro-Grids in South East Asia. OceanPixel
- [4] M.D. Bausas., O.D.G. de Luna and M.R.C.O. Aug. (2016). Tidal In-stream Energy Resource and Conversion Device Suitability Analysis in the Northern Philippines. Proceedings on Asian Conference on Remote Sensing.
- [5] Nevalainen, T (2016). The effect of unsteady sea conditions on tidal stream turbine loads and durability. PhD thesis. University of Strathclyde
- [6] Gracie-Orr, K (2017). A blade design methodology for overspeed power regulation of horizontal axis tidal turbines. PhD thesis. University of Strathclyde
- [7] Bartrop, N., Varyani, K.S., Grant, A., Clelland, D. and Pham X.P. (2017). Investigation into wave-current interactions in marine current turbines. Proceedings of IMechE 221 A: 223-241
- [8] Bahaj, A.S., Molland, A.F., Chaplin, J.R., and Batten, W.M.J. (2007) Power and Thrust measurement of marine current turbines under various hydrodynamic flow conditions in a cavitation tunnel and a towing tank. *Renewable Energy* 32: 407-426
- [9] Hau, E. (2006). *Wind Turbines, Fundamentals, Technologies, Application, Economics*, 2nd ed. Springer: Berlin, Germany
- [10] Habali, S., & Saleh, I. (2000). Local design, testing and manufacturing of small mixed airfoil wind turbine blades of glass fiber reinforced plastics. *Energy Conversion and Management*, 41(3), 249-280. doi:10.1016/S0196-8904(99)00103-x



Figure 7. Sample Visualization of how net loads are applied on the blade, x-axis is TSR and y-axis is higher loads

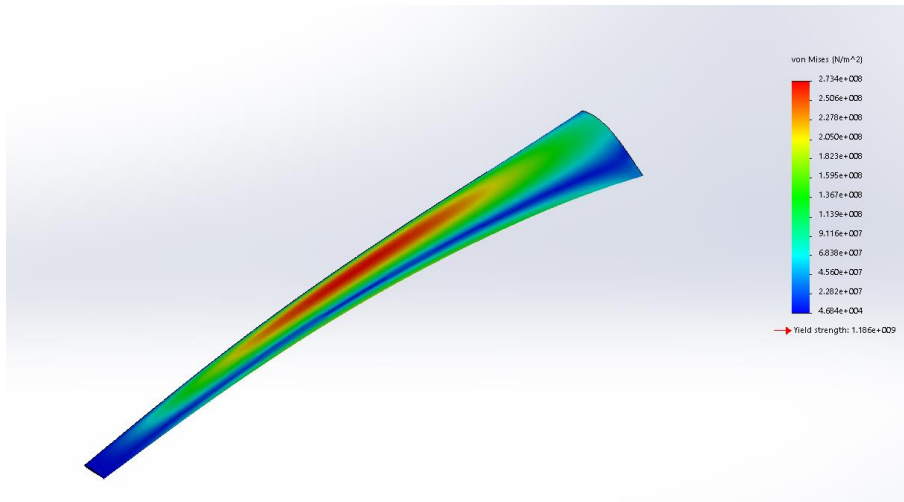


Figure 8. Stress distribution on the slender NACA hyperbolic chord distribution blade

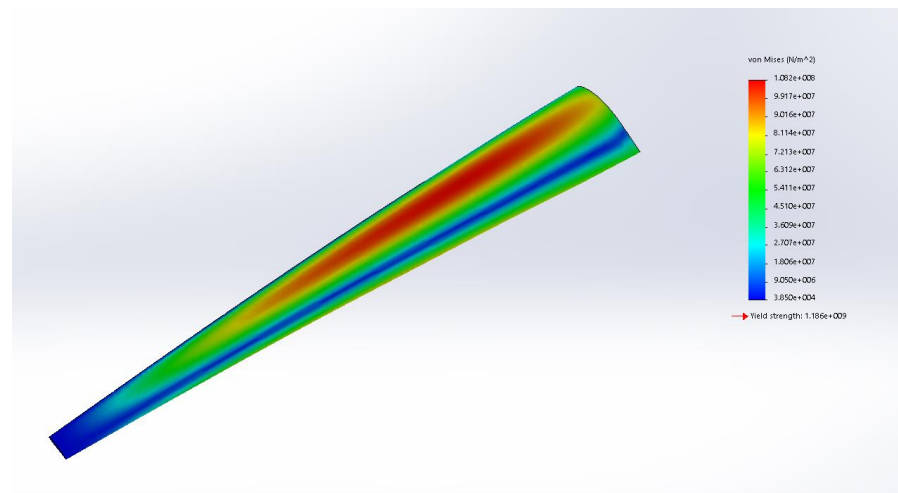


Figure 9. Stress distribution on the slender NACA base chord distribution blade

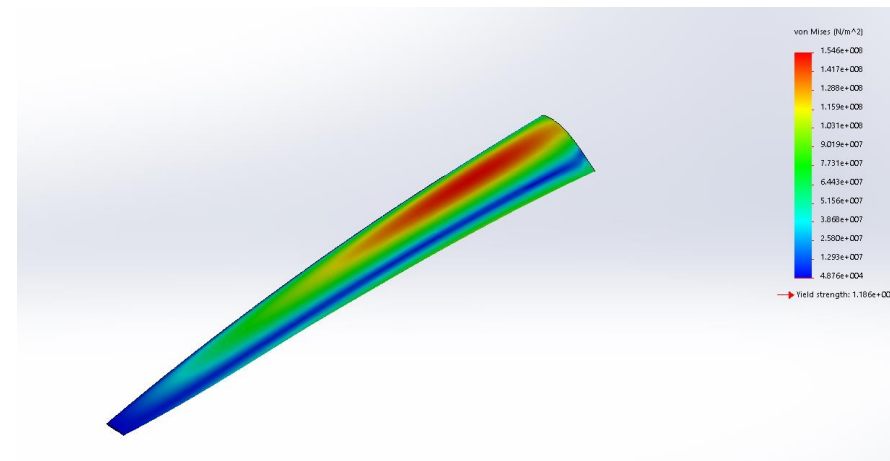


Figure 10. Stress distribution on the slender NACA elliptical chord distribution blade

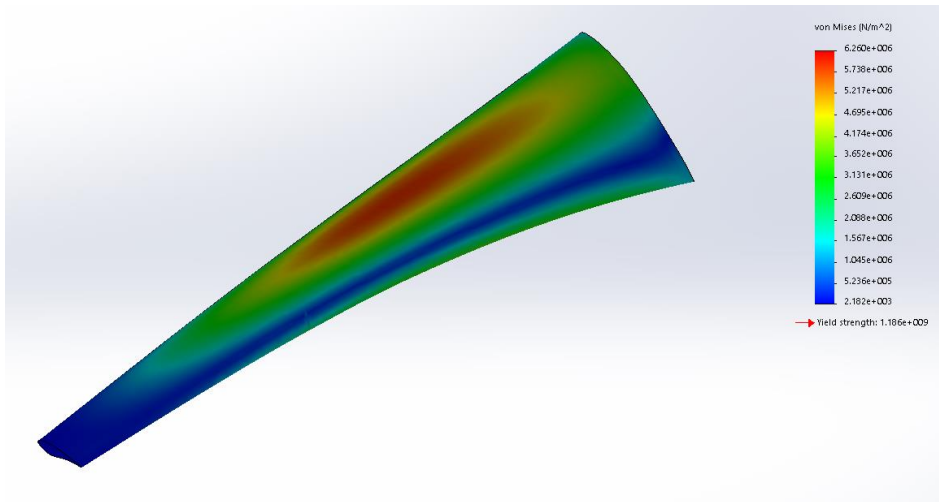


Figure 11. Stress distribution on the slender NREL hyperbolic chord distribution blade

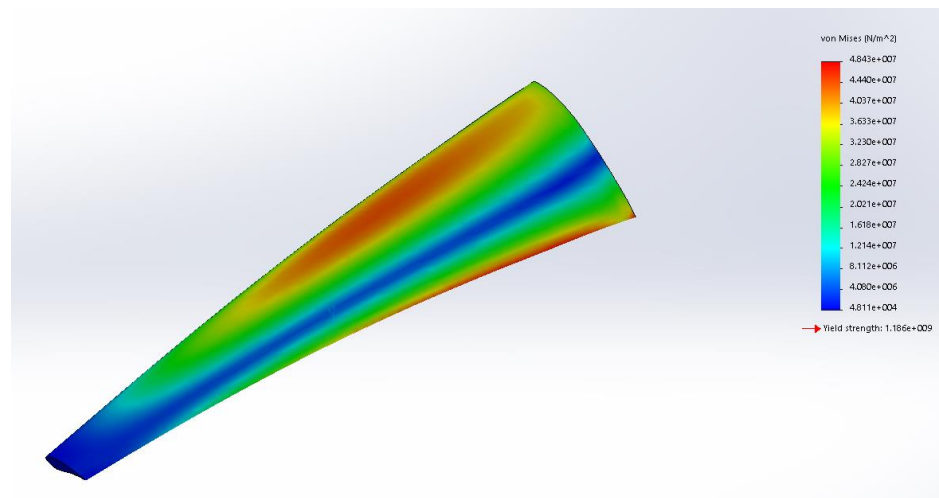


Figure 12. Stress distribution on the slender NREL base chord distribution blade

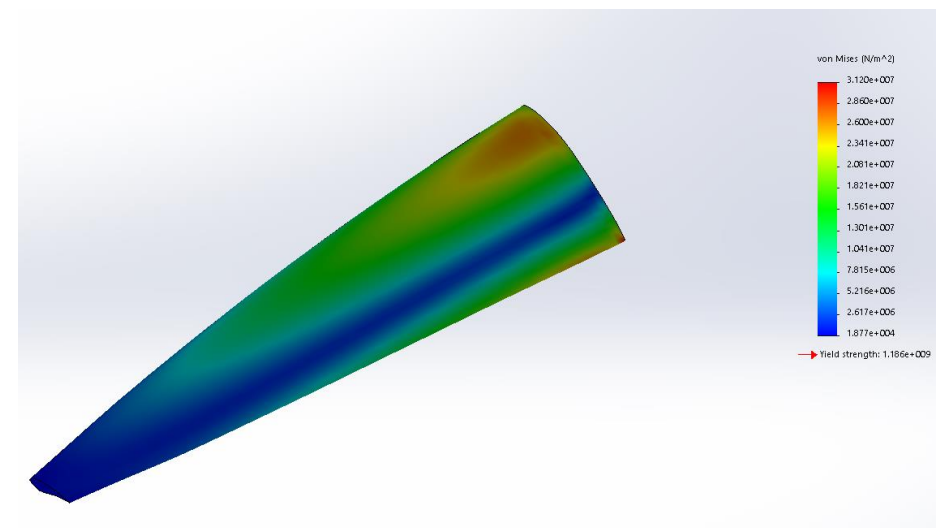


Figure 13. Stress distribution on the slender NREL elliptical chord distribution blade